UC Berkeley
UC Berkeley Previously Published Works

Title

Multidimensional genome-wide screening in yeast provides mechanistic insights into europium toxicity

Permalink

https://escholarship.org/uc/item/9tt764ps

Journal

Metallomics, 13(12)

ISSN

1756-5901

Authors

Pallares, Roger M
An, Dahlia D
Hébert, Solène
et al.

Publication Date

2021-12-06

DOI

10.1093/mtomcs/mfab061

Copyright Information

Peer reviewed

Multidimensional Genome-wide Screening in Yeast Provides Mechanistic Insights into Europium Toxicity

Roger M. Pallares,[1] Dahlia D. An,[1] Solène Hébert,[1] David Faulkner,[1] Alex Loguinov,[2] Michael Proctor,[2] Jonathan A. Villalobos,[1] Kathleen A. Bjornstad,[1] Chris J. Rosen,[1] Christopher Vulpe,[2] and Rebecca J. Abergel[1,3,*]

Affiliations:

[1]Chemical Sciences Division, Lawrence Berkeley National Laboratory, Berkeley, CA, 94720, USA

[2]Center for Environmental and Human Toxicology, Department of Physiological Sciences, College of Veterinary Medicine, University of Florida, Gainesville, FL, 32611, USA

[3]Department of Nuclear Engineering, University of California, Berkeley, CA, 94720, USA

*E-mail: abergel@berkeley.edu

Running head: Genome-wide study of europium toxicity in *S. cerevisiae*.

Abstract:

Europium is a lanthanide metal that is highly valued in optoelectronics. Even though europium is used in many commercial products, its toxicological profile has only been partially characterized, with most studies focusing on identifying lethal doses in different systems or bioaccumulation *in vivo*. This paper describes a genome-wide toxicogenomic study of europium in *Saccharomyces cerevisiae*, which shares many biological functions with humans. By using a multidimensional approach and functional and network analyses, we have identified a group of genes and proteins associated with the yeast responses to ameliorate metal toxicity, which include metal discharge paths through vesicle-mediated transport, paths to regulate

biologically-relevant cations, and processes to reduce metal-induced stress. Furthermore, the analyses indicated europium promotes yeast toxicity by disrupting the function of chaperones and cochaperones, which have metal-binding sites. Several of the genes and proteins highlighted in our study have human orthologues, suggesting they may participate in europium-induced toxicity in humans. By identifying the endogenous targets of europium as well as the already existing paths that can decrease its toxicity, we can determine specific genes and proteins that may help to develop future therapeutic strategies.

KEYWORDS: toxicogenomics, europium, lanthanides, toxicity, saccharomyces cerevisiae.

GRAPHICAL ABSTRACT:
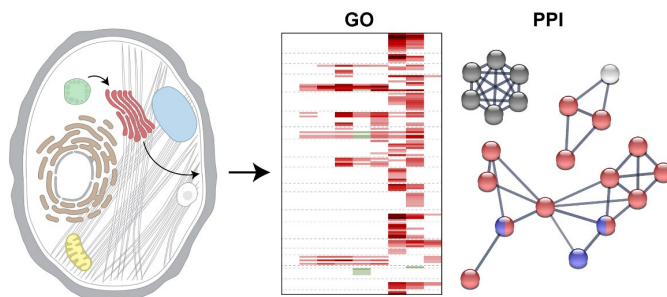
Introduction

Europium is a lanthanide metal that primarily adopts the +3 oxidation state.[1-3] The trivalent cation displays a characteristic red emission upon UV irradiation, where the positions of the emission peaks are largely unaffected by coordination.[3-5] Hence, Eu(III) ions are commonly used as dopant elements in glasses and matrices in photoelectronics,[6] with its main application being the doping of Y_2O_3 to form the red light-emitting $Y_2O_3:Eu^{3+}$ in chromatic lamps and projectors.[6,7] Before that, Eu(III) was commonly used in the cathodoluminescent $Y_2O_2S:Eu^{3+}$, which was present in cathode-ray tubes in color televisions and computer monitors.[6] Because Eu(III) emission originates from forbidden f−f transitions and direct electronic excitation is not efficient, the metal ion can alternatively be complexed with a light-harvesting ligand, which absorbs light and transfers the excitation energy to Eu(III).[8,9] Thus, Eu(III) complexes with chromophore-containing ligands are used as luminescent probes in bioassays.[10-13] Another interesting application of Eu(III) is in the production of anti-counterfeiting ink in Euro bank notes.[3]

Eu(III) applications in multiple industries have increased the risk of human exposure to the metal, especially in settings relevant to mining, processing, and recycling operations.[14-16] Hence, a deep understanding of Eu(III) biochemistry is necessary to minimize potential adverse health effects that may result from its use. However, the toxicological profile of Eu(III) has only been partially characterized, with most studies focusing on the identification of median lethal doses in different biological systems,[17-20] or the accumulation in tissues and organs *in vivo* after different exposure routes.[21,22] Although several studies have identified key proteins responsible for Eu(III) uptake and endogenous trafficking,[23-25] these studies did not determine the cellular functions disturbed by Eu(III) nor the biological responses activated to reduce Eu(III) toxicity.

Recently, our group employed a functional toxicogenomic approach in *Saccharomyces cerevisiae* to characterize toxicity mechanisms in the lanthanides series.[26] This strategy relies on the differential growth rates among deletion pools of mutants to assess the relationships between toxicant exposures and genes.[27,28] *S. cerevisiae* is one of the most commonly used biological systems because its genome is easily characterized by commercial techniques, and it shares many biological functions and pathways with humans.[29] In our previous work, we identified three distinctive trends within the lanthanide series, where deletions of key genes caused little to no effect on the cellular response to early lanthanides, while inducing high yeast sensitivity and resistance to mid and late lanthanides, respectively.[26] One of the breaking points in the trends was observed at Eu(III). Under the experimental conditions used in the previous study, Eu(III) affected the majority of yeast mutants in a non-specific manner (in contrast to the rest of the lanthanides whose toxicity was gene-specific), and no mechanistic information could be obtained for Eu(III). It is worth noting that europium has the most accessible divalent chemistry from all lanthanides,[30] which may favor its greater interaction with biological receptors. To overcome this issue and obtain mechanistic insights, we performed a multidimensional analysis where multiple conditions (*e.g.,* time of exposure and chemical dose) were systematically screened to identify both universal and condition-specific cellular responses to Eu(III).

Here, we report a genome-wide toxicogenomic study that characterizes the interaction mechanisms between Eu(III) and *S. cerevisiae*. The biological impact of the metal was concentration dependent, and a larger number of strains were disrupted as Eu(III) concentration increased. Functional and network analyses indicated that genes and proteins associated with several biological functions were necessary for yeast tolerance to the metal; these biological functions included vesicle-mediated transport through the Golgi apparatus and vacuole, ribosome assembly, sphingolipid biosynthesis, and mitochondria function. Additionally,

network analysis suggested that Eu(III) may disrupt the function of chaperones and cochaperones that have metal-binding sites, promoting toxicity in yeast cells. Lastly, several of the genes and proteins identified in our analyses are conserved in humans, and may play a role in the Eu(III) toxicity observed in humans.

METHODS

Materials

Europium (III) chloride hexahydrate 99%, magnesium (II) chloride 98%, hydrogen chloride 0.1 N and 6 N, sodium hydroxide 97%, potassium phosphate monobasic 98%, and sorbitol di-potassium hydrogen phosphate 98% were purchased from Sigma-Aldrich (St. Louis, MO). Milli-Q water was obtained from Millipore Milli-Q Integral 15 water purification system (Millipore Sigma, Burlington, MA). Europium solutions were prepared in 2 M HCl.

Yeast mutant strains and cultures

BY4743 background diploid yeast deletion strains (Life Technologies, Carlsbad, CA) were grown in yeast extract-peptone-dextrose media (YPD, containing 2% peptone, 2% dextrose, and 1% yeast extract) with continuous shaking (200 rpm) at 30 ˚C.

Wild-type yeast was grown to mid-log phase and subsequently diluted down to 0.0165 optical density at 600 nm (OD_{600}). Different Eu(III) treatments (ranging from 0 to 0.5 mM) were added to diluted yeast strains that were transferred into different wells in clear 96-well plates (Grenier Bio-One, Monroe, NC). Well plates containing the yeast were incubated at 30 ˚C with continuous 200 rpm shaking inside a Tecan Genios microplate reader (Tecan Group Ltd., Männedorf, Switzerland). OD_{600} of each well was measured every 15 min for a period of 24 h. IC_5, IC_{10} and IC_{20} concentrations (0.092, 0.108 and 0.131 mM, respectively) were calculated using the area under the curve.

Screening of the yeast genome

Homozygous diploid deletion pools (4291 mutants in total) were grown for 5, 10 and 15 generations in YPD medium at IC_5, IC_{10} and IC_{20} Eu(III) concentrations in an automated dispensing system robot built in-house.[31] The well plates containing the strains in YPD (700 ml in total) were continuously shaken and their OD_{600} was measured every 15 min. To prevent saturation and preserve the yeast in the log phase of growth, every 5 generations, an inoculant of 23 ml was added by the system robot to a fresh well of YPD. Once the strains were grown for 5, 10 or 15 generations, they were dispensed by the automated dispensing system to a cold plate to inhibit their growth, then centrifuged to remove the supernatant, frozen at -80 ˚C, and stored.[31]

Prior to use, the samples were thawed for 10 min, and the yeast pool pellets were re-suspended in autoclaved spheroplast buffer (2.62 g K_2HPO_4, 4.75 g KH_2PO_4, 109.3 g sorbitol, and 250 µL 1M $MgCl_2$). In order to lyse the cell wall, the strains were further incubated with Zymolyase (1 mg/ml, Zymo Research, Irvine, CA) for 2 hours at 37 ˚C.

DNA was extracted with the Corbett Robotics Xtractor-Gene robot and Qiagen DX regents (Qiagen, Hilden, Germany). Extracted DNA quality was assessed with a NanoQuant module (Tecan, Männedorf, Switzerland), which confirmed that the 260/280 nm ratios of extracted DNA ranged between 1.7 and 2.1, and the concentrations were between 20 and 100 ng/µL.

Next, polymerase chain reaction (PCR) was used to amplify the extracted DNA that contained the strain-specific barcodes, where 5 µL genomic DNA, 2 µL biotinylated primers that hybridize to universal sequences that flank the barcodes, and 22.5 µL of Platinum PCR SuperMix (Thermo Fisher Scientific, Waltham, MA) were mixed in sealed 96-well plates. The PCR program had the following cycle conditions: 95°C / 3min; 25 cycles of 94 °C / 30s, 55 °C / 30s, 72 °C / 30s; followed by 72°C / 10 min and hold at 10°C. Once the amplification step

was performed, the resulting DNA was purified and concentrated with ZR-96 DNA clean and concentrator-5 kit (Zymo Research, Irvine, CA), and the Quant-iT dsDNA Assay Kit (Thermo Fisher Scientific, Waltham, MA) was employed to quantify the oligonucleotides.

The purified and concentrated DNA solutions were run for 2 h in a 2% agarose gel to remove the primers, and then the DNA was cut in a UV box and extracted with GeneJet Gel Extraction Kit (Thermo Fisher Scientific, Waltham, MA). Finally, the DNA was sequenced at the Vincent J. Coates Genomics Sequencing Laboratory.

Barcode sequences that were significantly depleted in the treatment compared to the control pool at a given time point (log_2-ratio value < 0) identified genes whose mutation led to sensitive strains, whereas those that were significantly enriched (log_2-ratio value > 0) corresponded to genes whose deletion induced increased strain resistance to the treatment. A summary of sensitive and resistant strains was obtained by establishing a cutoff of 0.05 for false discovery rate (FDR) adjusted p-values.

Differential strain sensitivity analysis and functional analysis

Differential strain sensitivity analysis (DSSA) was performed as previously described.[26] A fitness score defined as the difference in the mean of the log_2 hybridization signal between Eu(III) treatment and control was used to identify strains with significant responses in the raw data (Dataset S1). The fitness score was calculated for each mutant to identify the strains that were statistically resistant or sensitive to Eu(III), where a negative score indicated the mutant was sensitive to the treatment, and the gene absent in that strain was likely required for tolerance to the metal. Similarly, a positive score showed the mutant was resistant to the treatment, and the absent gene product in that strain was likely impacted by Eu(III).

Gene ontology analysis was performed on the data obtained by DSSA with the David tool 6.7,[32] setting a FDR adjusted p-value cutoff of 0.05 (Dataset S2). FDR was used to correct the

p-values accounting for multiple-hypothesis testing.[33] Protein-protein interaction network analysis was performed by mapping the proteins coded by the deleted genes in the DSSA-identified mutants onto the STRING *S. cerevisiae* functional interaction network.[34] STRING provided a score (between 0.000 and 1.000) for every single interaction screened, which was proportional to the likelihood of that interaction being true-positive. We carried out the analysis by setting a score cutoff of 0.700, which was defined as "high-confidence" by the software.[34] The localization of the gene products identified in the protein-protein network analysis were screened in the Compartments[35] and UniProt[36] databases. Lastly, the Alliance of Genome Resources database was used to identify the human orthologues of genes highlighted in our analyses.[37]

Results and Discussion

Differential strain sensitivity analysis screened the genes required for sensitivity and tolerance to europium.

The Eu(III) concentrations that resulted in 5% (IC_5), 10% (IC_{10}), and 20% (IC_{20}) growth inhibition of the wild-type strain were initially determined (Figure S1). These concentrations are commonly used in functional toxicogenomics because they allow us to discern specific responses to chemicals instead of global non-specific cytotoxic effects.[27,28] A yeast pool of 4291 homozygous diploid deletion mutants were exposed to IC_5, IC_{10} and IC_{20} concentrations of Eu(III) for 5, 10 and 15 generations of growth, totaling nine experimental conditions in total. These different times of exposure allowed us to identify delayed-onset effects and biological responses that change over time.[27,28] Differential strain sensitivity analysis (DSSA)[38] was used to determine sensitive and resistant mutant strains to the metal, and their growth variations in $\log_2$ scale after the different exposures (Dataset S1). **Figure 1a** reports the total number of strains affected under each experimental condition, and shows two different trends when studying metal concentration effects. At lower Eu(III) concentrations (IC_5 and IC_{10}), only the growth of few strains (between 27 and 90) was disturbed, while at IC_{20}, the number of strains affected by the metal increased to between 2357 and 2686. These results seem to indicate that there is a concentration threshold, above which the biological impact of Eu(III) significantly increases. Notably, the percentage of resistant strains (compared to the total number of affected strains) increased at higher Eu(III) concentrations ($7 \pm 4\%$ at IC_5, $19 \pm 3\%$ at IC_{10}, and $44 \pm 2\%$ at IC_{20}). In resistant strains, we inferred the biological function coded by the absent gene was being directly or indirectly targeted by the metal causing yeast toxicity, and when the gene was removed, the resulting mutant had higher Eu(III) tolerance. In contrast, sensitive strains showed higher growth inhibition in the presence of the metal, suggesting that the biological function encoded by the absent gene was involved in processes responsible to ameliorate metal
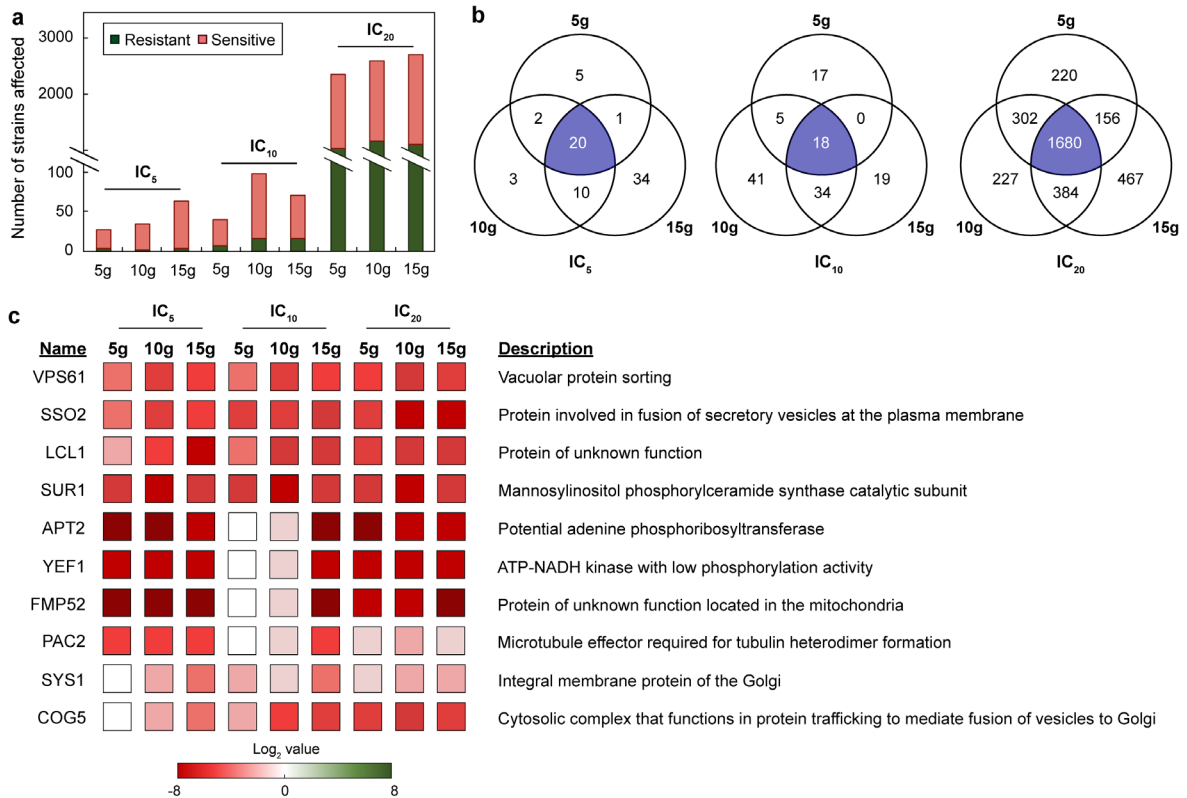
Figure 1. Resistant and sensitive mutants to Eu(III) identified by DSSA. (a) Total number of strains identified by DSSA after being exposed to IC_5, IC_{10}, and IC_{20} Eu(III) concentrations for 5, 10 and 15 generations. **(b)** Venn diagrams of disturbed mutants under different experimental conditions. **(c)** Top genes affected by europium, their growth variations in log_2 scale, and description of the proteins they encode.

toxicity, and when the gene was removed, the mutants became less tolerant to Eu(III) exposures. Thus, the results indicated that at low concentrations (IC_5, 92 μM Eu(III)), mostly genes responsible for detoxification pathways (*i.e.,* genes deleted in sensitive mutants) were statistically highlighted by the analysis, suggesting the yeast could bear metal exposures by activating those detoxification mechanisms. As Eu(III) concentration increased, so did the number of genes associated with metal-induced toxicity events (*i.e.,* genes deleted in resistant mutants). We inferred that at higher concentrations, the pathways that ameliorate the harmful effects of Eu(III) started to overload, and toxicity mechanisms were highlighted during the analysis.

Patterns among mutant strains were observed across the different time points as well. Although the number of disrupted strains increased along the number of generations exposed

to the metal, those effects were minor compared to the ones identified after concentration changes. **Figure 1b** illustrates this observation, where at fixed metal concentration, the majority of strains are disrupted at multiple time points. The top 10 strains that showed disrupted growth to the greatest number of experimental conditions are displayed in **Figure 1c**. Even though the genes deleted in these mutants were involved in multiple biological processes, three genes encoded enzymes and four encoded proteins responsible for transport between vesicles and organelles. The implications of these observations are discussed in the following sections.

The results displayed in Figure 1 were obtained in an in-house built automated system robot (refer to experimental section for further details) that performed the inhibition assays in competitive conditions.[31] We further confirmed our results by quantifying the growth inhibition of five representative mutants highlighted by DSSA, such as SSO2, SUR1, COG5, FIS1, and CSG2, in non-competitive conditions under IC_{20} Eu(III) concentrations. Both competitive and non-competitive assays yielded similar inhibition growths (Figure S2), corroborating our experimental set-up.

Functional analysis highlighted the biological attributes required for europium sensitivity and resistance.

Gene ontology (GO) enrichment analysis was applied to the strains identified by DSSA to determine if there were any overrepresented groups of genes (known as GO terms) that shared biological attributes.[39] Fewer numbers of overrepresented GO terms (FDR-adjusted p-value < 0.01) were observed at IC_5 and IC_{10} concentrations of Eu(III) compared to IC_{20} concentrations (**Figure 2**), corroborating the threshold hypothesis, where high metal concentrations (IC_{20}) triggered a greater number of yeast biological responses. Notably, even though resistant strains were as numerous as $44 \pm 2\%$ of all strains identified by DSSA at IC_{20} (Figure 1a), resistant

GO attributes were a small minority of the overrepresented GO terms in all tested conditions. This observation indicated that resistant mutations were not clustered around specific biological responses, but spread over the yeast genome, yielding only a few resistant GO terms as statistically significant. Almost all experimental conditions contained sensitive GO terms associated with vesicle-mediated transport, Golgi apparatus and vacuole, which were consistent with the top 10 strains that showed disrupted growth to the greatest number of experimental conditions plotted in Figure 1c. Regarding resistant GO terms, only a very few were highlighted by the functional analysis, such as terms associated with coated membranes. The predominance of vesicle-mediated transport, Golgi apparatus and vacuole attributes was also observed among the 15 most-overrepresented GO terms (Figure S3), of which nine were related to Golgi apparatus and vacuole, and four were related to vesicle-mediated transport categories.
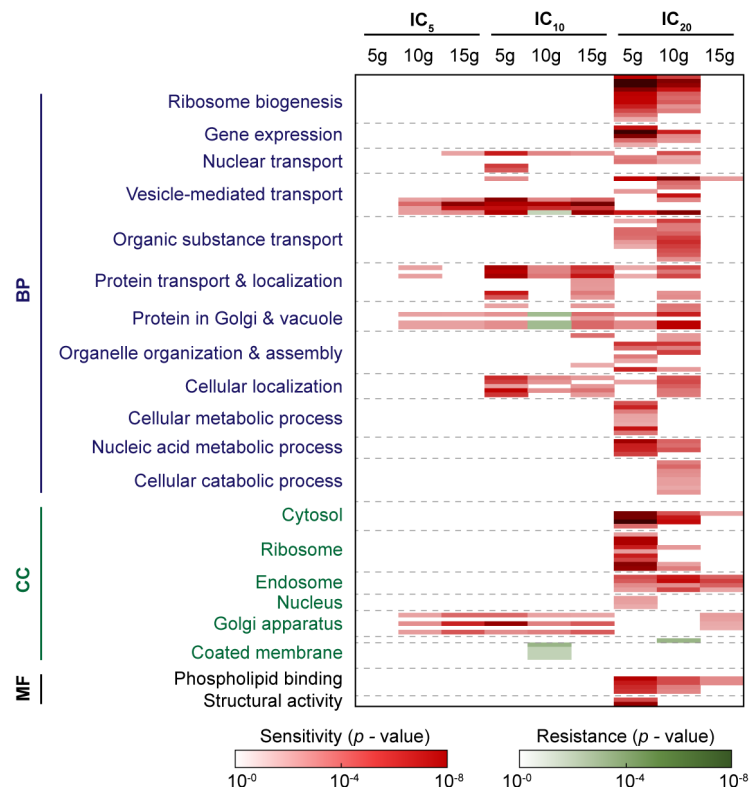

Figure 2. Gene ontology (GO) enrichment analysis of mutant strains identified by DSSA. Heat map of overrepresented GO terms and their FDR-adjusted *p*-value. The three GO domains are highlighted in the figure: biological process (BP), cellular component (CC), and molecular function (MF).

Protein-protein interaction network analysis identified the mechanisms responsible for yeast sensitivity and resistance to europium.

Once we had established that vesicle-mediated transport and Golgi apparatus and vacuole functions were some of the main functional categories disrupted by the metal, we performed protein-protein interaction network analysis to investigate whether the effects of Eu(III) were associated with specific protein interactions. The proteins encoded by the deleted genes in strains highlighted by DSSA were screened in the *S. cerevisiae* STRING database.[34] The network analysis was performed separately on the genes whose deletion promoted sensitivity or resistance, allowing us to distinguish detoxification responses and metal-mediated toxicity effects. The sensitivity network was made of several protein clusters in contrast to the resistance network, which only contained a protein pair.
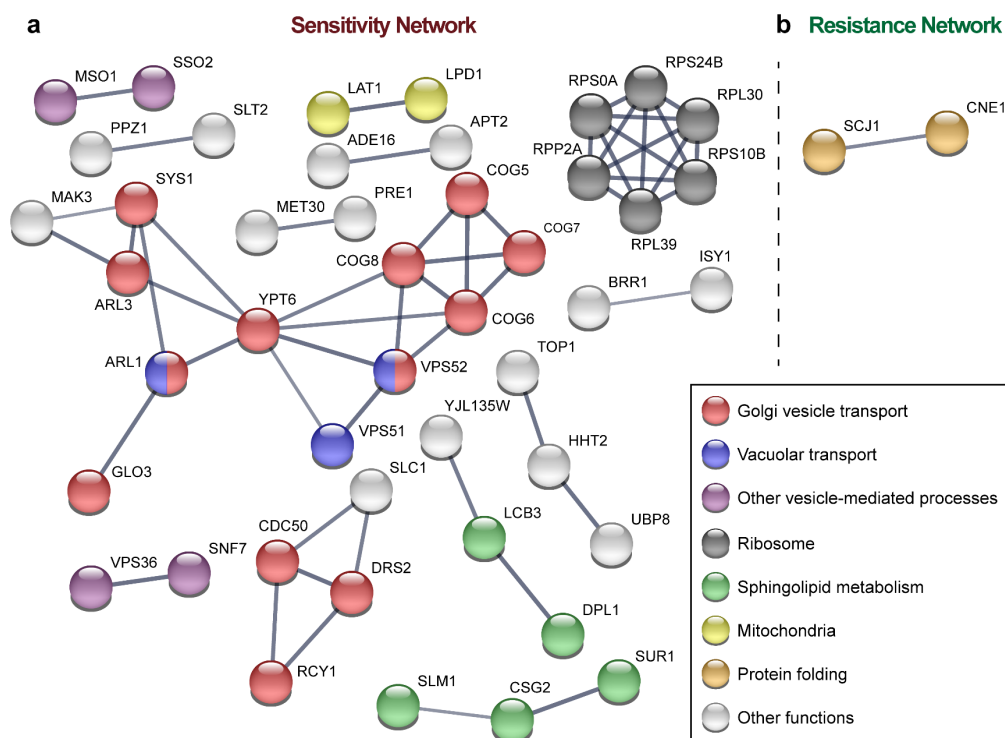

Figure 3. Protein-protein interaction network analysis identified mechanisms of europium interaction with yeast. Network of proteins coded by genes whose deletion promoted (**a**) sensitivity or (**b**) resistance to europium. All genes affected by at least 4 treatments were considered. Single proteins without any connection are not displayed for clarity. The protein-protein interaction network analysis was carried out with STRING software and a cutoff for confidence interactions of 0.70 (defined by the software as high confidence).

The largest cluster in the sensitivity network was constituted by proteins associated with Golgi vesicle transport and vacuolar transport (**Figure 3a**), corroborating our previous GO analysis (Figure 2). For instance, some of the proteins highlighted in that cluster included: COG5, COG6, COG7, and COG8, which are part of the conserved oligomeric Golgi (COG) complex, and participate in the fusion of vesicles to the Golgi apparatus and intra-Golgi trafficking;[40] VPS51 and VPS52, which code the GARP complex, and regulate retrograde traffic from endosomes to the Golgi apparatus and the vacuole targeting pathway in concert with YPT6 (also highlighted in the network analysis);[41,42] and ARL1 and ARL3, a group of GTPase enzymes that together with SYS1 mediate the Golgi-trafficking and vacuole-targeting pathways.[43,44] Moreover, ARL1 is also involved in the regulation of potassium cation influx into the cell. Taken together, the analysis identifying proteins associated with the Golgi apparatus and vacuole during the yeast response to Eu(III) is consistent with the role of these two organelles in intracellular storage of biologically-relevant cations and in transient storage during metal discharge.[45,46] Furthermore, some of the proteins forming the COG and GARP complexes have been associated with the yeast response to aluminum, manganese, zinc and cobalt, among others, and mutants lacking these proteins showed high metal sensitivity (and in some cases decreased metal efflux capabilities).[47,48] Outside the largest cluster, the sensitivity network had a protein pair formed by VPS36 and SNF7, which are part of the endosomal sorting complexes required for transport (ESCRT) system.[49] This protein system is involved in the formation of multi-vesicular bodies (a type of vesicle) and actively participates in preserving calcium homeostasis.[50] Notably, lanthanides have very similar coordination chemistry to calcium,[51] and bind to proteins with calcium-binding sites.[25,52,53] The ESCRT, GARP and COG complexes highlighted by the protein-protein network analysis are consistent with our previous toxicogenomic study, which identified these complexes as key components in the yeast response to several lanthanides.[26] Other proteins present in the sensitive network

that had not been previously associated with the yeast responses to the lanthanides include CDC50 and DRS2, which participate in the formation of transport vesicles, such as endosomes and post-Golgi exosomes.[54,55] Hence, CDC50 and DRS2 may be involved at both ends of the vesicle-mediated excretion pathway of the metal, first by transporting Eu(III) to the Golgi apparatus through vesicles, and later mediating in its efflux out of the cell post-Golgi processing. These two proteins also appear in the yeast response to other metals, such as zinc.[56] Another two proteins highlighted in the network that may also regulate the latter part of the metal discharge pathway are MSO1 and SSO2, which mediate vesicle fusion with cell membrane at exocytosis sites.[57,58]

In addition to proteins involved in vesicle-mediated transport, the sensitive network contained six ribosomal proteins (RPS0A, RPS10B, RPS224B, RPL30, RPL39 and RPP2A). Ribosomal protein production and assembly is a very complex process that requires the combination of multiple paths to preserve proteome homeostasis.[59] Although the exact mechanisms involved in its regulation are not fully understood, ribosomal protein production and assembly is partially controlled by stress signals, such as high concentration of metals.[59,60] Some ribosomal proteins highlighted in our network analysis (RPS10B and RPL39) have been associated with yeast responses to salt stress.[61] Another set of proteins highlighted in the sensitive network (CSG2, SUR1, DPL1, SLM1 and LCB3) were related to the biosynthesis of sphingolipids, a class of lipids that, in addition to their structural functions, mediate multiple biological processes, such as vesicle-mediated transport, ion signaling, and environmental stress resistance.[62] CSG2 and SUR1 participate in preserving calcium homeostasis,[63-65] while DPL1 regulates calcium influx through ion-channels.[65] Hence, mutations in the genes coding CSG2 and DPL1 have been associated with high intracellular accumulation of calcium.[63,66] Yeast using calcium-regulatory processes to ameliorate Eu(III) toxicity may be explained by both ions having similar coordination chemistry.[51] The other two proteins associated with

sphingolipid biosynthesis, SLM1 and LCB3, are essential for yeast survival under environmental stress.[67,68]

Lastly, a protein pair in the sensitive network was associated with mitochondria function. Particularly, LAT1 and LPD1 are part of the pyruvate dehydrogenase complex, which catalyzes the conversion of pyruvate to acetyl-CoA.[69,70] In the presence of heavy metals, the concentration of pyruvate in the mitochondria rises, disrupting the function of the organelle and increasing the levels of cytotoxic reactive oxygen species.[71] Thus, the presence of LAT1 and LPD1 in the sensitive network likely reflects the pyruvate dehydrogenase complex activity decreasing the levels of mitochondrial pyruvate caused by Eu(III), and preventing the over-generation of reactive oxygen species.

The protein-protein interaction network of genes whose deletion promoted resistance consisted of a single node pair (**Figure 5b**). The two proteins are a chaperone (CNE1) and a cochaperone (SCJ1) involved in protein folding.[72,73] CNE1 is the protein homolog of the mammalian calcium-binding calreticulin and calnexin,[74] while SCJ1 has a zinc-binding motif.[75,76] Therefore, we hypothesize that Eu(III) may bind to the calcium or zinc binding sites on these proteins, either causing aberrant activation of metal-regulated processes, or preventing normal protein function altogether.

Mapping the intracellular locations of the proteins identified in the network analysis allowed us to propose a mechanistic scheme to display the different yeast detoxification pathways (**Figure 4**). The most significant response seemed to be related to vesicle-mediated transport of Eu(III) using the Golgi apparatus and vacuole as transient storage prior to metal discharge through exocytosis. Other responses included proteins associated with sphingolipid-related functions, which were located in the endoplasmic reticulum and to a lesser extent in the vacuole, and LAT1 and LPD1, which likely decreased oxidative stress by reducing pyruvate levels in the mitochondria.
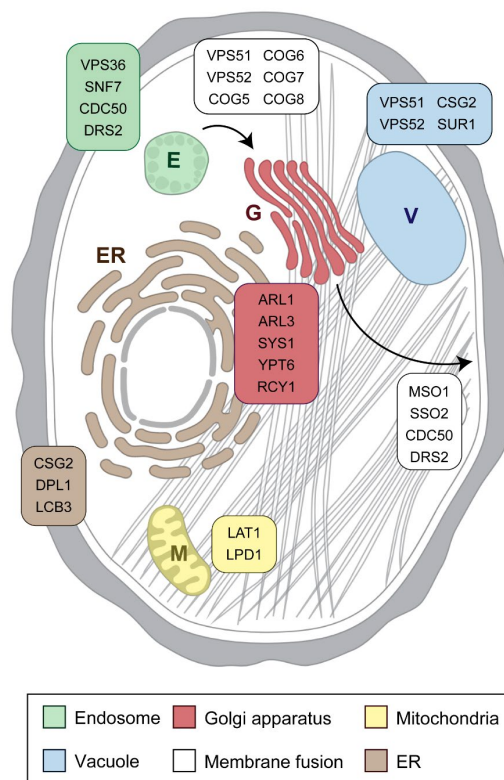
Figure 4. Intracellular localization of proteins that participate in yeast response to europium. The majority of the proteins were located in the endosomes. E, G, V, M and ER stand for endosome, Golgi apparatus, vacuole, mitochondria, and endoplasmic reticulum, respectively. The scheme of the yeast cell was obtained from Compartments.[35]

Lastly, the genes and proteins identified in the network analysis were screened in the Princeton Protein Orthology Database, and 33 human orthologues were identified (Table S1). Since many of the dysregulated biological functions identified in our study are preserved in humans, and multiple key proteins have human orthologues, those may also play a role in modulating Eu(III) toxicity in humans through processes similar to the ones identified in our analyses. Therefore, future toxicological studies in humans should consider these proteins as potential Eu(III) endogenous targets.

Conclusions

In summary, we have identified several gene networks associated with cellular responses to Eu(III), as well as the apparent biological functions disrupted by Eu(III) that promote

17

toxicity in *S. cerevisiae*. Multidimensional analysis showed a concentration threshold for Eu(III), wherein the growth of many more strains was affected at the IC_{20} concentration, compared to IC_5 and IC_{10} concentrations. GO analysis highlighted vesicle-mediated transport, Golgi apparatus and vacuole as the main functional categories associated with the yeast response to ameliorate Eu(III) toxicity. Protein-protein network analysis identified proteins related to vesicle-mediated transport through Golgi apparatus and vacuole, ribosomal assembly, sphingolipid biosynthesis and mitochondria function as key components of the yeast response to the metal. Some of these proteins participate in the regulation of biologically-relevant cations and the reduction of metal-induced stress. Protein-protein network analysis also pointed to Eu(III) disrupting the function of chaperons and cochaperones that have metal-binding sites, which could lead to cytotoxicity. Lastly, several of the genes and gene products identified in our analyses are conserved in humans, suggesting that those may also participate in Eu(III)-induced toxicity in humans. The identification of Eu(III) endogenous targets is a fundamental step in the future development of therapeutics.

ASSOCIATED CONTENT

Supporting Information.

Experimental Section; determination of IC_5, IC_{10} and IC_{20} concentrations of europium; non-competitive growth of representative mutants under IC_{20} concentrations of europium.

Notes

The authors declare no competing financial interest.

AUTHOR INFORMATION

Corresponding Author. *E-mail: abergel@berkeley.edu.

ORCID

Roger M. Pallares: 0000-0001-7423-8706

Dahlia D. An: 0000-0002-8763-6735

David Faulkner: 0000-0001-5532-2304

Rebecca J. Abergel: 0000-0002-3906-8761

References

(1) Cotton, S. Introduction to the Lanthanides. In *Lanthanide and Actinide Chemistry*; John Wiley & Sons: Hoboken, NJ, 2006; pp 1-7.

(2) Cotton, S. Coordination Chemistry of the Lanthanides. In *Lanthanide and Actinide Chemistry*; John Wiley & Sons: Hoboken, NJ, 2006; pp 35-60.

(3) Binnemans, K. Interpretation of europium(III) spectra. *Coord. Chem. Rev.* **2015,** *295*, 1-45.

(4) Vicentini, G.; Zinner, L. B.; Zukerman-Schpector, J.; Zinner, K. Luminescence and structure of europium compounds. *Coord. Chem. Rev.* **2000,** *196* (1), 353-382.

(5) Zurita, C.; Tsushima, S.; Bresson, C.; Garcia Cortes, M.; Solari, P. L.; Jeanson, A.; Creff, G.; Den Auwer, C. How Does Iron Storage Protein Ferritin Interact with Plutonium (and Thorium)? *Chem. Eur. J.* **2021,** *27* (7), 2393-2401.

(6) Feldmann, C.; Jüstel, T.; Ronda, C. R.; Schmidt, P. J. Inorganic Luminescent Materials: 100 Years of Research and Application. *Adv. Funct. Mater.* **2003,** *13* (7), 511-516.

(7) Binnemans, K.; Jones, P. T. Perspectives for the recovery of rare earths from end-of-life fluorescent lamps. *Journal of Rare Earths* **2014,** *32* (3), 195-200.

(8) Abergel, R. J.; D'Aléo, A.; Ng Pak Leung, C.; Shuh, D. K.; Raymond, K. N. Using the Antenna Effect as a Spectroscopic Tool: Photophysics and Solution Thermodynamics of the Model Luminescent Hydroxypyridonate Complex [EuIII(3,4,3-LI(1,2-HOPO))]−. *Inorg. Chem.* **2009,** *48* (23), 10868-10870.

(9) Pallares, R. M.; Sturzbecher-Hoehne, M.; Shivaram, N. H.; Cryan, J. P.; D'Aléo, A.; Abergel, R. J. Two-Photon Antenna Sensitization of Curium: Evidencing Metal-Driven Effects on Absorption Cross Section in f-Element Complexes. *J. Phys. Chem. Lett.* **2020,** *11* (15), 6063-6067.

(10) Heffern, M. C.; Matosziuk, L. M.; Meade, T. J. Lanthanide Probes for Bioresponsive Imaging. *Chem. Rev.* **2014,** *114* (8), 4496-4539.

(11) Pallares, R. M.; An, D. D.; Tewari, P.; Wang, E. T.; Abergel, R. J. Rapid Detection of Gadolinium-Based Contrast Agents in Urine with a Chelated Europium Luminescent Probe. *ACS Sensors* **2020,** *5* (5), 1281-1286.

(12) Pallares, R. M.; Carter, K. P.; Zeltmann, S. E.; Tratnjek, T.; Minor, A. M.; Abergel, R. J. Selective Lanthanide Sensing with Gold Nanoparticles and Hydroxypyridinone Chelators. *Inorg. Chem.* **2020,** *59* (3), 2030-2036.

(13) Pallares, R. M.; Agbo, P.; Liu, X.; An, D. D.; Gauny, S. S.; Zeltmann, S. E.; Minor, A. M.; Abergel, R. J. Engineering Mesoporous Silica Nanoparticles for Targeted Alpha Therapy against Breast Cancer. *ACS Appl. Mater. Interfaces* **2020,** *12* (36), 40078-40084.

(14) Shumilin, E.; Rodríguez-Figueroa, G.; Sapozhnikov, D. Lanthanide Contamination and Strong Positive Europium Anomalies in the Surface Sediments of the Santa Rosalía Copper Mining Region, Baja California Peninsula, Mexico. *Bull. Environ. Contam. Toxicol.* **2005,** *75* (2), 308-315.

(15) Dawood, Y. H.; Abd El-Naby, H. H.; Sharafeldin, A. A. Influence of the alteration processes on the origin of uranium and europium anomalies in trachyte, central Eastern Desert, Egypt. *J. Geochem. Explor.* **2004,** *81* (1), 15-27.

(16) Pallares, R. M.; Hébert, S.; Sturzbecher-Hoehne, M.; Abergel, R. J. Chelator-assisted high performance liquid chromatographic separation of trivalent lanthanides and actinides. *New J. Chem.* **2021,** *45* (32), 14364-14368.

(17) Haley, T. J.; Komesu, N.; Colvin, G.; Koste, L.; Upham, H. C. Pharmacology and Toxicology of Europium Chloride. *J. Pharm. Sci.* **1965,** *54* (4), 643-645.

(18) Tai, P.; Zhao, Q.; Su, D.; Li, P.; Stagnitti, F. Biological toxicity of lanthanide elements on algae. *Chemosphere* **2010,** *80* (9), 1031-1035.

(19) Gonzalez, V.; Vignati, D. A. L.; Leyval, C.; Giamberini, L. Environmental fate and ecotoxicity of lanthanides: Are they a uniform group beyond chemistry? *Environment International* **2014,** *71*, 148-157.

(20) Rim, K. T.; Koo, K. H.; Park, J. S. Toxicological Evaluations of Rare Earths and Their Health Impacts to Workers: A Literature Review. *Safety and Health at Work* **2013,** *4* (1), 12-26.

(21) Ogawa, Y.; Suzuki S Fau - Naito, K.; Naito K Fau - Saito, M.; Saito M Fau - Kamata, E.; Kamata E Fau - Hirose, A.; Hirose A Fau - Ono, A.; Ono A Fau - Kaneko, T.; Kaneko T Fau - Chiba, M.; Chiba M Fau - Inaba, Y.; Inaba, Y.; et al. Toxicity study of europium chloride in rats. *Journal of environmental pathology, toxicology and oncology* **1995,** *14* (1), 1-9.

(22) Bingham, D.; Dobrota, M. Distribution and excretion of lanthanides: comparison between europium salts and complexes. *BioMetals* **1994,** *7*, 142-148.

(23) Tikhonova, T. N.; Shirshin, E. A.; Budylin, G. S.; Fadeev, V. V.; Petrova, G. P. Assessment of the Europium(III) Binding Sites on Albumin Using Fluorescence Spectroscopy. *J. Phys. Chem. B* **2014,** *118* (24), 6626-6633.

(24) Barkleit, A.; Heller, A.; Ikeda-Ohno, A.; Bernhard, G. Interaction of europium and curium with alpha-amylase. *Dalton Trans.* **2016,** *45* (21), 8724-8733.

(25) Pallares, R. M.; Panyala, N. R.; Sturzbecher-Hoehne, M.; Illy, M.-C.; Abergel, R. J. Characterizing the general chelating affinity of serum protein fetuin for lanthanides. *J. Biol. Inorg. Chem.* **2020,** *25* (7), 941-948.

(26) Pallares, R. M.; Faulkner, D.; An, D. D.; Hébert, S.; Loguinov, A.; Proctor, M.; Villalobos, J. A.; Bjornstad, K. A.; Rosen, C. J.; Vulpe, C.; Abergel, R. J. Genome-wide toxicogenomic study of the lanthanides sheds light on the selective toxicity mechanisms associated with critical materials. *Proc. Natl. Acad. Sci.* **2021,** *118* (18), e2025952118.

(27) Gaytán, B. D.; Loguinov, A. V.; Peñate, X.; Lerot, J.-M.; Chávez, S.; Denslow, N. D.; Vulpe, C. D. A Genome-Wide Screen Identifies Yeast Genes Required for Tolerance to Technical Toxaphene, an Organochlorinated Pesticide Mixture. *PLoS One* **2013,** *8* (11), e81253.

(28) North, M.; Tandon, V. J.; Thomas, R.; Loguinov, A.; Gerlovina, I.; Hubbard, A. E.; Zhang, L.; Smith, M. T.; Vulpe, C. D. Genome-Wide Functional Profiling Reveals Genes Required for Tolerance to Benzene Metabolites in Yeast. *PLoS One* **2011,** *6* (8), e24205.

(29) Karathia, H.; Vilaprinyo, E.; Sorribas, A.; Alves, R. Saccharomyces cerevisiae as a Model Organism: A Comparative Study. *PLoS One* **2011,** *6* (2), e16015.

(30) Dau, P. D.; Shuh, D. K.; Sturzbecher-Hoehne, M.; Abergel, R. J.; Gibson, J. K. Divalent and trivalent gas-phase coordination complexes of californium: evaluating the stability of Cf(ii). *Dalton Trans.* **2016,** *45* (31), 12338-12345.

(31) Proctor, M.; Urbanus, M. L.; Fung, E. L.; Jaramillo, D. F.; Davis, R. W.; Nislow, C.; Giaever, G. The Automated Cell: Compound and Environment Screening System (ACCESS) for Chemogenomic Screening. In *Yeast Systems Biology: Methods and Protocols*; Castrillo, J. I.; Oliver, S. G., Eds.; Humana Press: Totowa, NJ, 2011; pp 239-269.

(32) Dennis, G.; Sherman, B. T.; Hosack, D. A.; Yang, J.; Gao, W.; Lane, H. C.; Lempicki, R. A. DAVID: Database for Annotation, Visualization, and Integrated Discovery. *Genome Biology* **2003,** *4* (9), R60.

(33) Benjamini, Y.; Hochberg, Y. Controlling the False Discovery Rate: A Practical and Powerful Approach to Multiple Testing. *Journal of the Royal Statistical Society: Series B (Methodological)* **1995,** *57* (1), 289-300.

(34) Szklarczyk, D.; Franceschini, A.; Wyder, S.; Forslund, K.; Heller, D.; Huerta-Cepas, J.; Simonovic, M.; Roth, A.; Santos, A.; Tsafou, K. P.; Kuhn, M.; Bork, P.; Jensen, L. J.;

von Mering, C. STRING v10: protein–protein interaction networks, integrated over the tree of life. *Nucleic Acids Res.* **2014,** *43* (D1), D447-D452.

(35) Binder, J. X.; Pletscher-Frankild, S.; Tsafou, K.; Stolte, C.; O'Donoghue, S. I.; Schneider, R.; Jensen, L. J. COMPARTMENTS: unification and visualization of protein subcellular localization evidence. *Database* **2014,** *2014*.

(36) The UniProt, C. UniProt: a hub for protein information. *Nucleic Acids Res.* **2015,** *43* (D1), D204-D212.

(37) The Alliance of Genome Resources, C. Alliance of Genome Resources Portal: unified model organism research platform. *Nucleic Acids Res.* **2020,** *48* (D1), D650-D658.

(38) Jo, W. J.; Loguinov, A.; Wintz, H.; Chang, M.; Smith, A. H.; Kalman, D.; Zhang, L.; Smith, M. T.; Vulpe, C. D. Comparative Functional Genomic Analysis Identifies Distinct and Overlapping Sets of Genes Required for Resistance to Monomethylarsonous Acid (MMAIII) and Arsenite (AsIII) in Yeast. *Toxicol. Sci.* **2009,** *111* (2), 424-436.

(39) Eden, E.; Navon, R.; Steinfeld, I.; Lipson, D.; Yakhini, Z. GOrilla: a tool for discovery and visualization of enriched GO terms in ranked gene lists. *BMC Bioinformatics* **2009,** *10* (1), 48.

(40) Whyte, J. R. C.; Munro, S. Vesicle tethering complexes in membrane traffic. *J. Cell Sci.* **2002,** *115* (13), 2627.

(41) Eising, S.; Thiele, L.; Fröhlich, F. A systematic approach to identify recycling endocytic cargo depending on the GARP complex. *eLife* **2019,** *8*, e42837.

(42) Suda, Y.; Kurokawa, K.; Hirata, R.; Nakano, A. Rab GAP cascade regulates dynamics of Ypt6 in the Golgi traffic. *Proc. Natl. Acad. Sci.* **2013,** *110* (47), 18976.

(43) Jackson, C. L. Membrane Traffic: Arl GTPases Get a GRIP on the Golgi. *Curr. Biol.* **2003,** *13* (5), R174-R176.

(44) Setty, S. R. G.; Strochlic, T. I.; Tong, A. H. Y.; Boone, C.; Burd, C. G. Golgi targeting of ARF-like GTPase Arl3p requires its Nα-acetylation and the integral membrane protein Sys1p. *Nat. Cell Biol.* **2004,** *6* (5), 414-419.

(45) Reddi, A. R.; Jensen, L. T.; Culotta, V. C. Manganese Homeostasis in Saccharomyces cerevisiae. *Chem. Rev.* **2009,** *109* (10), 4722-4732.

(46) Liu, W. Control of Calcium in Yeast Cells. In *Introduction to Modeling Biological Cellular Control Systems*; Liu, W., Ed.; Springer Milan: Milano, 2012; pp 95-122.

(47) Kakimoto, M.; Kobayashi, A.; Fukuda, R.; Ono, Y.; Ohta, A.; Yoshimura, E. Genome-Wide Screening of Aluminum Tolerance in Saccharomyces cerevisiae. *BioMetals* **2005,** *18* (5), 467-474.

(48) Bleackley, M. R.; Young, B. P.; Loewen, C. J. R.; MacGillivray, R. T. A. High density array screening to identify the genetic requirements for transition metal tolerance in Saccharomyces cerevisiae. *Metallomics* **2011,** *3* (2), 195-205.

(49) Saksena, S.; Sun, J.; Chu, T.; Emr, S. D. ESCRTing proteins in the endocytic pathway. *Trends Biochem. Sci.* **2007,** *32* (12), 561-573.

(50) Jo, W. J.; Loguinov, A.; Chang, M.; Wintz, H.; Nislow, C.; Arkin, A. P.; Giaever, G.; Vulpe, C. D. Identification of Genes Involved in the Toxic Response of Saccharomyces cerevisiae against Iron and Copper Overload by Parallel Analysis of Deletion Mutants. *Toxicol. Sci.* **2007,** *101* (1), 140-151.

(51) Cotruvo, J. A. The Chemistry of Lanthanides in Biology: Recent Discoveries, Emerging Principles, and Technological Applications. *ACS Central Science* **2019,** *5* (9), 1496-1506.

(52) Brayshaw, L. L.; Smith, R. C. G.; Badaoui, M.; Irving, J. A.; Price, S. R. Lanthanides compete with calcium for binding to cadherins and inhibit cadherin-mediated cell adhesion. *Metallomics* **2019,** *11* (5), 914-924.

(53) Edington, S. C.; Gonzalez, A.; Middendorf, T. R.; Halling, D. B.; Aldrich, R. W.; Baiz, C. R. Coordination to lanthanide ions distorts binding site conformation in calmodulin. *Proc. Natl. Acad. Sci.* **2018,** *115* (14), E3126.

(54) Sakane, H.; Yamamoto, T.; Tanaka, K. The Functional Relationship between the Cdc50p-Drs2p Putative Aminophospholipid Translocase and the Arf GAP Gcs1p in Vesicle Formation in the Retrieval Pathway from Yeast Early Endosomes to the TGN. *Cell Structure and Function* **2006,** *31* (2), 87-108.

(55) Gall, W. E.; Geething, N. C.; Hua, Z.; Ingram, M. F.; Liu, K.; Chen, S. I.; Graham, T. R. Drs2p-Dependent Formation of Exocytic Clathrin-Coated Vesicles In Vivo. *Curr. Biol.* **2002,** *12* (18), 1623-1627.

(56) Pagani, M. A.; Casamayor, A.; Serrano, R.; Atrian, S.; Ariño, J. Disruption of iron homeostasis in Saccharomyces cerevisiae by high zinc levels: a genome-wide study. *Mol. Microbiol.* **2007,** *65* (2), 521-537.

(57) Weber, M.; Chernov, K.; Turakainen, H.; Wohlfahrt, G.; Pajunen, M.; Savilahti, H.; Jäntti, J. Mso1p Regulates Membrane Fusion through Interactions with the Putative N-Peptide–binding Area in Sec1p Domain 1. *Mol. Biol. Cell* **2010,** *21* (8), 1362-1374.

(58) Marash, M.; Gerst, J. E. t-SNARE dephosphorylation promotes SNARE assembly and exocytosis in yeast. *The EMBO Journal* **2001,** *20* (3), 411-421.

(59) Albert, B.; Kos-Braun, I. C.; Henras, A. K.; Dez, C.; Rueda, M. P.; Zhang, X.; Gadal, O.; Kos, M.; Shore, D. A ribosome assembly stress response regulates transcription to maintain proteome homeostasis. *eLife* **2019,** *8*, e45002.

(60) Shcherbik, N.; Pestov, D. G. The Impact of Oxidative Stress on Ribosomes: From Injury to Regulation. *Cells* **2019,** *8* (11).

(61) Posas, F.; Chambers, J. R.; Heyman, J. A.; Hoeffler, J. P.; de Nadal, E.; Ariño, J. n. The Transcriptional Response of Yeast to Saline Stress*. *J. Biol. Chem.* **2000,** *275* (23), 17249-17255.

(62) Dickson, R. C. Roles for Sphingolipids in Saccharomyces cerevisiae. In *Sphingolipids as Signaling and Regulatory Molecules*; Chalfant, C.; Poeta, M. D., Eds.; Springer New York: New York, NY, 2010; pp 217-231.

(63) Beeler, T.; Gable, K.; Zhao, C.; Dunn, T. A novel protein, CSG2p, is required for Ca2+ regulation in Saccharomyces cerevisiae. *J. Biol. Chem.* **1994,** *269* (10), 7279-7284.

(64) To, K. K.-W.; Tsang, O. T.-Y.; Yip, C. C.-Y.; Chan, K.-H.; Wu, T.-C.; Chan, J. M.-C.; Leung, W.-S.; Chik, T. S.-H.; Choi, C. Y.-C.; Kandamby, D. H.; Lung, D. C.; Tam, A. R.; Poon, R. W.-S.; Fung, A. Y.-F.; Hung, I. F.-N.; Cheng, V. C.-C.; Chan, J. F.-W.; Yuen, K.-Y. Consistent Detection of 2019 Novel Coronavirus in Saliva. *Clinical Infectious Diseases* **2020**, 10.1093/cid/ciaa149.

(65) Schneiter, R. Brave little yeast, please guide us to Thebes: sphingolipid function in S. cerevisiae. *BioEssays* **1999,** *21* (12), 1004-1010.

(66) Birchwood, C. J.; Saba, J. D.; Dickson, R. C.; Cunningham, K. W. Calcium Influx and Signaling in Yeast Stimulated by Intracellular Sphingosine 1-Phosphate Accumulation*. *J. Biol. Chem.* **2001,** *276* (15), 11712-11718.

(67) Daquinag, A.; Fadri, M.; Jung, S. Y.; Qin, J.; Kunz, J. The yeast PH domain proteins Slm1 and Slm2 are targets of sphingolipid signaling during the response to heat stress. *Mol. Cell. Biol.* **2007,** *27* (2), 633-650.

(68) Ferguson-Yankey, S. R.; Skrzypek, M. S.; Lester, R. L.; Dickson, R. C. Mutant analysis reveals complex regulation of sphingolipid long chain base phosphates and long chain bases during heat stress in yeast. *Yeast* **2002,** *19* (7), 573-586.

(69) Steensma, H. Y.; Holterman, L.; Dekker, I.; van Sluis, C. A.; Wenzel, T. J. Molecular cloning of the gene for the E1α subunit of the pyruvate dehydrogenase complex from Saccharomyces cerevisiae. *Eur. J. Biochem.* **1990,** *191* (3), 769-774.

(70) Matsuda, F.; Ishii, J.; Kondo, T.; Ida, K.; Tezuka, H.; Kondo, A. Increased isobutanol production in Saccharomyces cerevisiae by eliminating competing pathways and resolving cofactor imbalance. *Microbial Cell Factories* **2013,** *12* (1), 119.

(71) Lee, J.-Y.; Ishida, Y.; Takahashi, T.; Naganuma, A.; Hwang, G.-W. Transport of pyruvate into mitochondria is involved in methylmercury toxicity. *Sci. Rep.* **2016,** *6* (1), 21528.

(72) Xu, X.; Kanbara, K.; Azakami, H.; Kato, A. Expression and Characterization of Saccharomyces cerevisiae Cne1p, a Calnexin Homologue. *The Journal of Biochemistry* **2004,** *135* (5), 615-618.

(73) Payne, T.; Finnis, C.; Evans, L. R.; Mead, D. J.; Avery, S. V.; Archer, D. B.; Sleep, D. Modulation of Chaperone Gene Expression in Mutagenized Saccharomyces cerevisiae Strains Developed for Recombinant Human Albumin Production Results in Increased Production of Multiple Heterologous Proteins. *Appl. Environ. Microbiol.* **2008,** *74* (24), 7759.

(74) De Virgilio, C.; Bürckert, N.; Neuhaus, J.-M.; Boller, T.; Wiemken, A. CNE1, a Saccharomyces cerevisiae Homologue of the Genes Encoding Mammalian Calnexin and Calreticulin. *Yeast* **1993,** *9* (2), 185-188.

(75) Silberstein, S.; Schlenstedt, G.; Silver, P. A.; Gilmore, R. A Role for the DnaJ Homologue Scj1p in Protein Folding in the Yeast Endoplasmic Reticulum. *J. Cell Biol.* **1998,** *143* (4), 921-933.

(76) Ellis, C. D.; Wang, F.; MacDiarmid, C. W.; Clark, S.; Lyons, T.; Eide, D. J. Zinc and the Msc2 zinc transporter protein are required for endoplasmic reticulum function. *J. Cell Biol.* **2004,** *166* (3), 325-335.